# Assortativity decreases the robustness of interdependent networks

Di Zhou,[1] H. Eugene Stanley,[1] Gregorio D'Agostino,[2] and Antonio Scala[3,4]

[1]*Center for Polymer Studies and Department of Physics, Boston University, Boston, Massachusetts 02215, USA*
[2]*ENEA-CR "Casaccia," via Anguillarese 301, I-00123 Roma, Italy*
[3]*ISC-CNR Dipartimento di Fisica, Sapienza Università di Roma, Piazzale Moro 5, 00185 Roma, Italy*
[4]*London Institute of Mathematical Sciences, 22 South Audley St., Mayfair, London W1K 2NY, United Kingdom*

It was recently recognized that interdependencies among different networks can play a crucial role in triggering cascading failures and, hence, systemwide disasters. A recent model shows how pairs of interdependent networks can exhibit an abrupt percolation transition as failures accumulate. We report on the effects of topology on failure propagation for a model system consisting of two interdependent networks. We find that the internal node correlations in each of the two interdependent networks significantly changes the critical density of failures that triggers the total disruption of the two-network system. Specifically, we find that the assortativity (i.e., the likelihood of nodes with similar degree to be connected) within a single network decreases the robustness of the entire system. The results of this study on the influence of assortativity may provide insights into ways of improving the robustness of network architecture and, thus, enhance the level of protection of critical infrastructures.

## I. INTRODUCTION

The quality of life in modern society strongly depends on the effective delivery of basic services as water, electricity, and communications; the infrastructures providing these basic services are, therefore, called critical infrastructures. Indeed, maintaining every critical infrastructure (CI) is a growing challenge for modern society. Of great interest is the interdependence of CIs. One clear example of this interdependence is the "binomial" system in which electrical power networks depend on telecommunication networks and vice versa. Understanding cascading failure in interdependent networks is a problem currently receiving much attention. For example, failure propagation is a common phenomenon that can lead to such catastrophic effects as the remarkable September 2003 total blackout across Italy [1].

One approach to understanding failure propagation is to develop a simulation of an entire system that takes into account all of the details associated with the system. Although some remarkable results have been achieved for selected regions when all the information is available [2], these simulations are not useful in understanding the mechanisms that induce cascading effects. Because of the huge amount of data involved, such an approach requires heroic efforts, even when considering a simple system [3]. Frequently privacy constraints or difficulties in accessing or probing the system of interest become factors, and often an adequate amount of information is not available. Thus, other approaches are needed to understand the fundamental issues underlying cascading effects.

Here we will use the complex network paradigm to acquire some understanding of possible CI vulnerabilities to help focus more detailed analyses [4]. For example, the complex network paradigm can address the problem of interdependencies among CIs. It was recently demonstrated [5] that when the degree of interdependence between networks is increased, the robustness of the system to cascade failures decreases [6] and vice versa.

Besides the natural applications to the protection of CIs, the analysis of the properties of interdependent networks is a subject of growing interest in many scientific fields, ranging from public cooperation [7] to epidemic spreading [8–11] to human physiology [12].

Although previous research has indicated how to mitigate systemic risk by tuning network interdependencies [13], the role of topology of each component network has yet to be investigated. The interdependency level among a set of networks can be fixed—because of economic or technological constraints—and, thus, may be untunable.

If we know the average degree of a network, degree correlation becomes the simplest parameter for classifying the internal network topology. Using the interacting failure model (IFM) for a two-layered network system (2LNS) [6], we find that assortativity decreases the robustness to random failure. In particular, by considering both Erdős-Rényi (ER) and scale-free (SF) networks, we find that assortativity causes a sharp increase in the fragility of coupled networks with a node distribution described by a power law.

In Sec. II we review the concept of assortativity, describe the methods employed to generate sample networks with different assortativity coefficients, and review the two-layer network model of cascading failures. In Sec. III we present the results of our simulations, which we then discuss in Sec. IV.

## II. METHODS

A fundamental quantity characterizing the structure and driving the behavior of a large network is the probability distribution function $P(k)$ of node degree $k$ [14,15]. It has been shown that both humanly constructed and natural networks are often characterized by a $P(k)$ with heavy tails leading to unforeseen effects, e.g., the disappearance of epidemic thresholds [16]. Other quantities, e.g., the local density of triangles, the modular structure, communities, and motifs, can be used to further characterize network structure [14].

Assortativity is the tendency of entities to seek out and group with those other entities that exhibit similar characteristics. In networks, assortativity is the tendency of neighbor nodes to have similar degrees and, thus, to be measurable

using link-averaged degree pair correlation [17]. Using a physical approach, we improve the one-point average-degree characterization of a network by considering assortativity, a two-point correlation quantity.

The assortativity coefficient $r$ is defined in terms of the correlation between the degrees of neighboring vertices

$$r \equiv \frac{\langle jk \rangle_e - [\langle (j+k)/2 \rangle_e]^2}{\langle (j^2+k^2)/2 \rangle_e - [\langle (j+k)/2 \rangle_e]^2}, \tag{1}$$

where the averages $\langle \cdots \rangle_e$ are evaluated over all edges $e$ and $j,k$ are the degrees of the adjacent vertices associated with edge $e$. High values of the assortativity ($r \sim 1$) imply that neighboring nodes have similar degrees, while low values ($r \sim -1$) imply that high-degree nodes tend to be connected to low-degree ones; random pairing corresponds to $r \sim 0$.

An alternative form for this expression has been given by Newman [17],

$$r = \frac{\sum_{jk} jk(e_{jk} - q_j q_k)}{\sum_k [k^2 q_k - (kq_k)^2]}, \tag{2}$$

in terms of the normalized degree distribution $q_k = (k+1)P(k+1)/\sum_k kP(k)$ and the joint probability distribution $e_{ij}$ (i.e., the two point function) of the residual degrees at the either ends of a randomly chosen edge.

For a single stand-alone network, increasing the assortativity makes it more robust against node removal [18,19] and, in general, stronger with respect to diffusion-driven dynamical processes [20]. On the other hand, assortativity makes networks more unstable [21], as measured by the May criterion [22], and, in general, less controllable [20,23].

### A. Varying the assortativity

We next demonstrate how assortativity affects cascading fault propagation in interdependent networks by tuning $r$ while keeping the degree distribution fixed. To produce networks of varying assortativity, several methods (mostly based on link swapping [24]) have been employed, like accepting assortative moves with a given probability $p$ [25]. We believe that the most flexible way of sampling of the space of possible networks is to introduce a simple Hamiltonian [20,26], as it allows us to apply all the standard tools of statistical mechanics.

Following Ref. [20], we first define **A**, the adjacency matrix associated with the network (an $N \times N$ matrix exhibiting a unitary value $A_{ij} = 1$ when node $i$ is linked to node $j$ and vanishing elsewhere). Next, we define a statistical ensemble in which the probability measure $\mu(G) \propto \exp[-J\,H(G)]$ of a given graph $G$ is induced by the Hamiltonian

$$\mathcal{H}(G) \equiv \sum_{ij} k_i A_{ij} k_j. \tag{3}$$

Here $k_i$ is the degree of node $i$, and the "coupling constant" $J$ may assume both positive and negative values. Such a Hamiltonian is a simple quadratic form in the node degrees resembling strictly the form applied to model classical spin systems.

Note that for a given $P(k)$ the terms $\langle (j+k)/2 \rangle_e$ and $\langle (j^2+k^2)/2 \rangle_e$ in Eq. (1) do not depend on how nodes are linked, but that the term $\langle jk \rangle_e$ is directly related to the Hamiltonian as
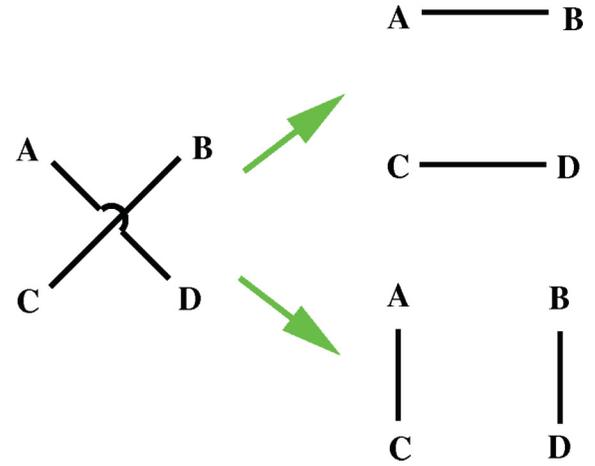


FIG. 1. (Color online) The link-swap procedure consists in deleting two edges $AB$ and $CD$ and adding either the edges $AC,BD$ or the edges $AD,BD$ respecting constraints like the absence of multiple links. Such a procedure always leaves the number of links attached to each node unchanged and, therefore, it leaves the degrees of the nodes unchanged.

$\mathcal{H} \propto \langle k_i k_j \rangle$. Thus large values of $J$ will favor graphs with large values of $r$ and vice versa.

Such a Hamiltonian has been recently explored by Yook and Park [27], who have found that the network configuration sampled at equilibrium satisfy the power-law distribution $P(k) \sim k^{-3/2}$. We instead explore the configuration space defined by link swapping: In this way, not only the initial $P(k)$ but also each node degree is kept constant (see Fig. 1). In order to sample configurations according to $\mu(G)$, we set the link swapping probability to be $e^{-J,\Delta\mathcal{H}}$. Although link-swap moves can be assortative, disassortative, or neutral [28], in our case assortative and disassortative configurations will be preferentially sampled according to the sign of $J$ with a monotonically increasing sampling of the assortativity $r$ with respect to the parameter $J$ [20].

In order to examine the effects of assortativity for both SF and ER networks, we use both the Barabasi-Albert (BA) [29] and the ER [30] model networks as starting configurations for link-swapping Monte Carlo (MC) dynamics. We find that in ER networks MC equilibrium is reached with a number of steps per node apparently independent of the number of nodes [26] but that in SF networks the situation is more complicated. We find that in BA networks the range of assortativities reached in a given number of steps shrinks as the system size increases [31]. Thus, similar allocated simulation times allow us to explore a smaller assortativity range for BA networks than for ER networks.

### B. Interdependent failures model

To model interdependent networks with assortativity we use the IFM of Ref. [6]. In the original IFM there are two spatial networks (ICT and power distribution) and only the geographically nearest nodes interact. We consider two networks $A$ and $B$ that have the same number of nodes $N$ and that share the same topology, and thus the same assortativity (or disassortativity). We consider a case in which a unique node

$b_i$ in network $B$ corresponds to a unique node $a_i$ in network $A$, i.e., $a_i$ and $b_i$ have a mutual dependence. In the IFM, in order for node $a_i$ to function properly, node $b_i$ must also function properly and vice versa. If $b_i$ becomes dysfunctional, $a_i$ will also become dysfunctional. This interdependence relation can be described as a bidirectional link $a_i \leftrightarrow b_i$ between $a_i$ and $b_i$. Thus, each $a_i$ node in network $A$ has a corresponding counterpart $b_i$ node in network $B$.

To model random attack or failure, we randomly remove a fraction $1 - x$ of nodes from network $A$ ($x$ is the fraction of initially surviving nodes). Because of the interdependence between the two networks, the nodes in network $B$ that depend on the removed $A$ nodes are also removed. When the nodes and links in network $B$ are removed, network $B$ may break up into several connected components ("clusters"). We assume that only the nodes belonging to the largest cluster (the so-called giant component) continue to be functional [6] and remove the nodes from $B$ that do not belong to this giant component. Because of mutual interdependency, removing the $B$ nodes in network $B$ not in the giant component will cause the removal of the corresponding $A$ nodes in network $A$. This iterative process generates a cascade of failures that continues until node elimination ceases. At that point, if the two networks still have giant components, they will be the same size. The algorithm used in this procedure consists of the following steps:

*s0:* Remove the fraction $1 - x$ of initial failed nodes in layer $A$

*s1:* Identify the largest component $S_A$

*s2:* Remove the $n_A$ nodes of $A$ not in $S_A$

*s3:* Remove the $n_B$ nodes of $B$ not linked to $S_A$

*s4:* Identify the largest component $S_B$

*s5:* Remove the $n_B$ nodes of $B$ not in $S_B$

*s6:* Remove the $n_A$ nodes of $A$ not linked to $S_B$

*s7:* If $n_A > 0$, then repeat from *s1*

*s8:* Output the final survived giant components $S_A$ and $S_B$

Such algorithms can be rephrased in terms of the fixpoint of an operator. In fact, let us define $Q_A$ as the operator that selects the largest component of network $A$ and let $P_{AB}$ the operator that select the subnetwork of $A$ linked to the existing nodes of $B$. The final result of the cascading algorithm then is the fixpoint of the operator,

$$G = P_{AB} \circ Q_B \circ P_{AB} \circ Q_A. \qquad (4)$$

The characterization of the operator $G$ in terms of generating functions is the starting point for the current analytical threatments of the IFM model [6]; it has yet to be investigated whether a generalization of such an approach would allow us to take into account the role of the assortativity.

In general, even if for simple percolation the method of generating functions is still applicable for the case of varying assortativity, the functions to be calculated have rarely an analytical closed form. Numerical simulations therefore seem to be the main method used to study the effects of assortativity in model systems.

For ER and BA networks, the IFM exhibits an abrupt transition [6] at an *a priori* unknown value of $x = x_c$. When a fraction of nodes larger than $1 - x_c$ is initially attacked or fails and, hence, is removed, the system experiences cascading disruption and (when the iterative process stops) ends up

completely fragmented, and the relative size of the giant component tends to vanish. When a fraction of nodes equal to or less than $1 - x_c$ is attacked or fails, there is always a finite fraction of nodes surviving, i.e., the giant component relative size does not vanish.

### C. Percolation

In classical percolation [32], increasing the fraction of removed nodes $1 - x$ reduces the size (i.e., the number of nodes) $S$ of the largest cluster. In the thermodynamic limit $N \to \infty$ (where $N$ is the number of nodes) the process experiences a phase transition, i.e., the fraction of nodes $s \equiv S/N$ belonging to the largest component drops to $s = 0$ for $x < x_c$. For $x > x_c$, $s$ is nonzero. Depending on the order of the transition, a discontinuous jump is observed in the order parameter $s$ or in one of its derivatives with regard to $x$. Finite-size effects round out the behavior of $s$ and make it difficult to distinguish a genuine weak first-order transition (small jump in $s$) from a second-order transition [33]. Although the sharpness of the transition for the IFM indicates the possibility that IFM experiences a first-order percolation transition [6], much care must be used in assessing the transition order for a given network [34]. We want to remark that, while classical percolation can be described in terms of thermodynamical equilibrium states, this does not seem to be the case for the IFM model. Nevertheless, both percolation and IFM share analogous concepts and even techniques (like the use of generating functions to produce approximate analytical solutions); therefore, all the standard machinery of percolation comes handy in analyzing and understanding the IFM.

We simulate the IFM and calculate the size of the largest cluster ("giant component") $S$ at varying values of the fraction $x$ of initially surviving nodes. As an order parameter for the percolation transition, we focus on the fraction of nodes $s \equiv S/N$ belonging to the giant component. We indicate by $\langle s \rangle$ the value of $s$ averaged both over different layers of the same average assortativity (the same $J$) and over different IFM simulations.

Next we estimate the percolation threshold $x_c$ corresponding to different assortativities (i.e., different $J$ values) using two methods:

I: We calculate the point of maximum fluctuation

$$\langle (\delta s)^2 \rangle \equiv \langle s^2 \rangle - \langle s \rangle^2 \qquad (5)$$

of the giant component, which is expected to be large for both first- and second-order transitions [33].

II: In order to compare the estimates of $x_c$ obtained by use of Method I, we must also consider the numerical derivative

$$\Delta \langle s \rangle \equiv \frac{\langle s(x + \epsilon) \rangle - \langle s(x - \epsilon) \rangle}{2\epsilon} \qquad (6)$$

in the critical region, and we use $\epsilon = 10^{-3}$; such a choice is dictated from the fact that the derivatives do not show appreciable numerical changes for smaller values of $\epsilon$. In classical percolation $\Delta \langle s \rangle$ is equivalent to $\langle (\delta s)^2 \rangle$,

$$\Delta \langle s \rangle \approx \partial_x \langle s \rangle \propto \langle (\delta s)^2 \rangle \qquad (7)$$

for a second-order transition, and it measures the jump $\langle s(x_c^+) \rangle - \langle s(x_c^-) \rangle$ at $x = x_c$ in the order parameter near a

first-order transition

$$\epsilon \Delta \langle s(x_c) \rangle \approx \langle s(x_c^+) \rangle - \langle s(x_c^-) \rangle, \tag{8}$$

where

$$\langle s(x_c^\pm) \rangle \equiv \lim_{\epsilon \to 0} \langle s(x_c \pm \epsilon) \rangle \tag{9}$$

are the values just before and after the discontinuity.

Due to the finite-size effect, the $x_c$ values found using these two methods may differ, but as system size increases we expect the corresponding $x_c$ values from the two methods to converge.

## III. RESULTS

### A. Generating the networks

To generate networks with varying assortativity, we start with a network with a given degree distribution $P(k)$ and apply MC rewiring for different values of $J$ according to the sampling probability $\exp[-J\,H(G)]$ [20]. Negative values of $J$ lead to a disassortative network, and positive values to an assortative network. In other words, when employing a positive $J$, rewiring connecting nodes of similar degree are accepted more frequently, whereas when employing a negative $J$, rewiring connecting nodes of very different degrees are preferred. The absolute value of $J$ behaves like an inverse temperature: the higher its value, the stronger the selection. In order to improve the statistics over the configurations, we start with uncorrelated initial conditions (i.e., we restart the procedure from scratch) and generate 100 independent networks for each value of $J$.

We duplicate each configuration to create two topologically identical monolayers ($A$ and $B$). Linking each node in layer $A$ to one and only one node in layer $B$ provides the 2LNS we will employ in our IFM simulations. To avoid correlations among the degrees of the two layers, we first perform a random permutation of the labels of one of the two layers and then create a connection $A_i \leftrightarrow B_i$ that represents the mutual dependence of the nodes. For each 2LNS, we perform 100 independent simulations of the IFM model. Thus, for each $J$ we perform $10^4$ simulations starting from 100 different initial networks.

To compare the ER case with the SF case, we generate in both cases networks with $N = 10\,000$ nodes and an average degree $\langle k \rangle = 6$. To generate ER networks (ERnets) with varying assortativity, we employ 17 different $J$ values that produce networks with an average assortativity that ranges from $r = -0.8$ to $r = 0.8$. To generate SF networks (SFnets) with varying assortativity, we use the Barabasi-Albert network [29], employ eight different $J$ values, and produce networks with an average assortativity that ranges from $-0.12$ to $0.16$.

### B. Breakdown of coupled SF networks

We simulate the IFM and calculate the fraction of nodes belonging to the giant component. Figure 2 shows the behavior of the order parameter $\langle s \rangle$ as a function of the fraction of survived nodes for the SFnets. Note that the size of the giant component increases significantly in a limited region that depends on the assortativity; in a system of finite size, this is an indication for a percolation phase transition. Two different regions of stability can be identified that correspond to the two different phases, (i) a percolative phase in which the
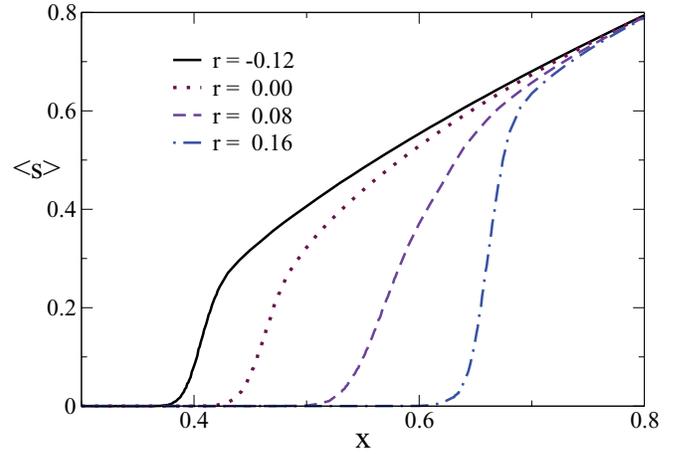


FIG. 2. (Color online) Fraction $\langle s \rangle$ of sites in the giant component as a function of the fraction $x$ of initially undamaged nodes for $N = 10\,000$ scale-free networks. Curves are obtained by averaging 1000 simulations over 100 independent networks for each value of $x$.

giant component includes a number of nodes proportional to $N$ ($S \sim N$, i.e., a nonvanishing $s$) and (ii) a broken phase in which the largest component is negligible [$S \sim o(N)$, i.e., $s \sim 0$]. The amount of damage needed to destroy the giant component decreases with assortativity, and we find the sharpness of the transition to decrease at fixed system size.

Such an effect can be understood by observing that the breakdown process consists in repeated applications of a percolation algorithm on single networks. In the case of a single network [17] increasing the assortativity reduces the extension of the largest component. In other words, at each iteration, the fraction of removed nodes (complementary to the giant component) increases; thus, the iterations over the two networks amplify the effect of the assortativity easing the breakdown of the coupled system.

To estimate the percolation threshold $x_c$ that corresponds to different $J$ values (i.e., to the different assortativities $r$), we calculate the point of maximum fluctuation for the size of the giant component. Figure 3 shows the fluctuations of the largest component $\langle (\delta s)^2 \rangle$ in a SFnet as a function of $x$ for sample values of the SFnet. To attain a better estimate $x_c$, we perform more simulations in the region where the maximum of $\langle (\delta s)^2 \rangle$ is attained.

Figure 4 shows that the numerical derivative $\Delta \langle s \rangle$ also shows a peak in the critical region. Note that one may also estimate the critical threshold as the inflection point of the largest component profiles, i.e., from the peak of the numerical derivative $\Delta \langle s \rangle$. Nevertheless, no significant difference is observed within the accuracy of our simulations, i.e., the inflection points of $\langle s \rangle$ coincide, within the error bars, with a maximum of $\langle (\delta s)^2 \rangle$.

Using the two methods above (via the peak of $\langle (\delta s)^2 \rangle$ or via the peak of $\Delta \langle s \rangle$), we can obtain the dependence of the percolation threshold $x_c$ on the assortativity $r$. Figure 5 shows data for the SFnets and provides evidence that the percolation threshold is an increasing function of the assortative coefficient $r$; therefore, robustness decreases with increasing assortativity.

As a general result, it has been observed that a phase transition in a numerical model often coincides with a peak in
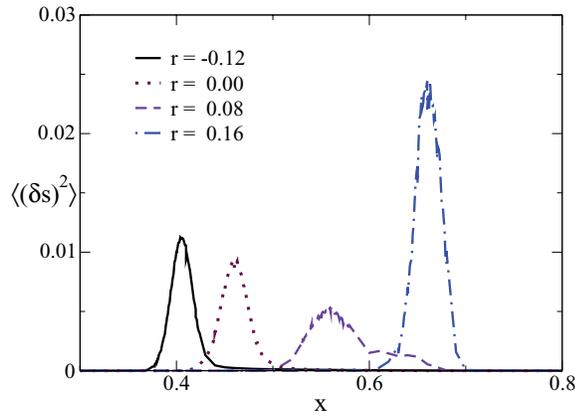
FIG. 3. (Color online) Fluctuations $\langle(\delta s)^2\rangle$ of the order parameter $s$ as a function of the fraction $x$ of the initially undamaged nodes for $N = 10\,000$ scale-free networks. The position of the peak for $\langle(\delta s)^2\rangle$ can be used to estimate the critical fraction of nondamaged sites $x_c$. Curves are obtained by averaging 1000 simulations over 100 independent networks for each value of $x$.



FIG. 5. (Color online) Estimated values of the percolation threshold $x_c$ as a function of the assortativity coefficient $r$ for $N = 10\,000$ scale-free networks. The values of $x_c$ are estimated as the maxima of $\langle(\delta s)^2\rangle$, as well as the peaks of the $\Delta\langle s\rangle$ profiles. Note that the two estimates are very close for disassortative nets but differ a bit more for assortative nets.

the number of operations required to calculate the significant quantities (order parameters and potentials). In our case, the number of iterations (NOI) needed for the IFM algorithm to converge represents a natural measure for the computing operations. Consistent with the general principle, Fig. 6 shows that the NOI for the IFM algorithm exhibits a peak close to the critical threshold. As a possible interpretation, we note that the NOI represents the sum of a set of stochastic variables (one for each iteration) that are null when the removal of nodes does not fragment the giant component and are unitary elsewhere. Therefore, the NOI measures the stability of the largest component on further node removal.

As mentioned above, we generate ER networks with the same average degree. Thus, configurations with a given size $N$ and a given assortativity $r$ are distinguishable only by their degree distributions. So if we plot the properties of networks of the same size versus $r$, we can pinpoint and compare the
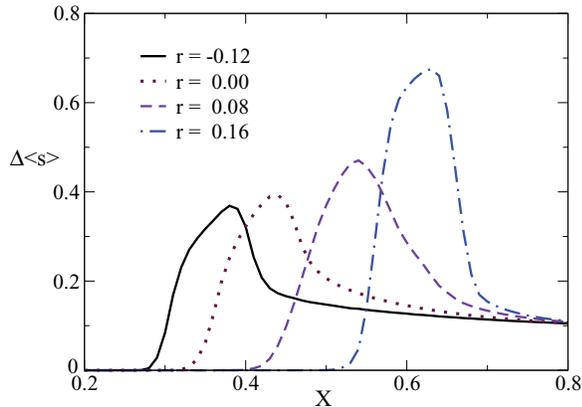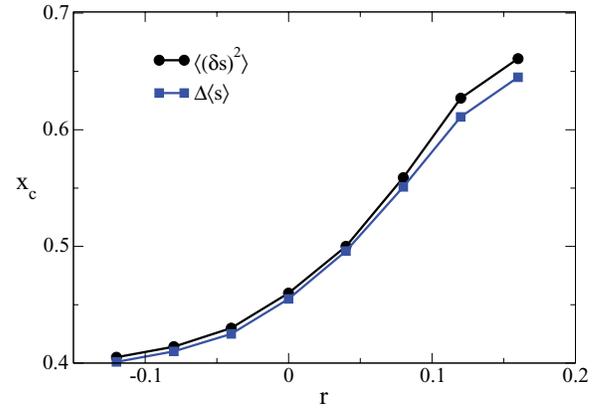
difference between the behavior of ER and SF networks. In Fig. 7 we show that the phase transition requires an increasing number of damaged sites with increasing assortativity for ERnets as well. Unlike SFnets, the effect on the critical threshold in ERnets is much more limited. In Fig. 8 we compare the estimated thresholds in the two cases. It is clear that in a SFnet the critical threshold $x_c$ varies dramatically but that in a ERnet it is almost flat. This effect of enhanced response to assortativity in the SFnets with respect to the ERnets is consistent to what is observed in single-layer networks [20].

### C. Order of the phase transition

It is difficult to determine the order of a phase transition from simulations. To see whether this kind of phase transition is first order or second order, we analyze the fluctuations of the size of the giant component.

In fact, for a second-order transition the divergence of the fluctuations $\langle(\delta s)^2\rangle$ at $x_c$ would be signaled at finite system



FIG. 4. (Color online) Normalized numerical increment $\Delta\langle s\rangle$ of the order parameter $s$ as a function of the fraction $x$ of initially undamaged nodes for $N = 10\,000$ scale-free networks. In conventional percolation $\Delta\langle s\rangle \sim \langle\delta s\rangle$ can be used to estimate the the critical fraction of damaged sites $x_c$. Curves are obtained by averaging 1000 simulations over 100 independent networks for each value of $x$.
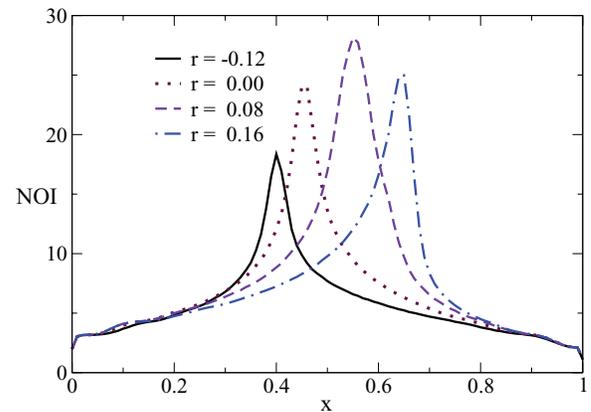


FIG. 6. (Color online) Number of iterations (NOI) for the IFM algorithm to converge as a function of the initially undamaged node fraction. Peak positions for different assortative coefficients are close to $x_c$ as estimated from $\langle(\delta s)^2\rangle$.
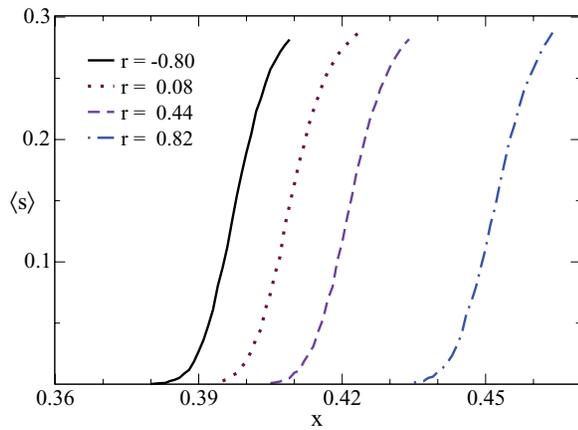
FIG. 7. (Color online) Fraction $\langle s \rangle$ of sites in the largest component as a function of the fraction $x$ of initially undamaged nodes for $N = 10\,000$ Erdős-Rényi networks. Curves are obtained by averaging for each $x$ value $10^4$ simulations over 100 independent networks.

sizes by an increase in the peak of $\langle (\delta s)^2 \rangle$ and by the narrowing of the width of the peak. In Fig. 9 we show that, although there is a slight narrowing of the peaks with system size, there is no sign of a second-order divergence. Figure 7 shows the fluctuation profiles for SFnets for different sizes ($N = 5000$, $10\,000$, and $14\,000$). We find analogous results for ERnets.

To further check whether this kind of phase transition is first order or second order, we analyze the size of the second-largest cluster $S_2$ and its counterpart, $s_2 \equiv S_2/N$. In a second-order transition, the presence of a sharp peak in $s_2$ is coupled to a sharp increase of $s$ near $x = x_c$. In fact, at criticality, the size of the second percolating cluster has the same scaling as the giant component [35] also for systems above the critical dimension [36]. On the other hand, first-order transitions are characterized by finite-size clusters and by $S_2/N \to 0$.
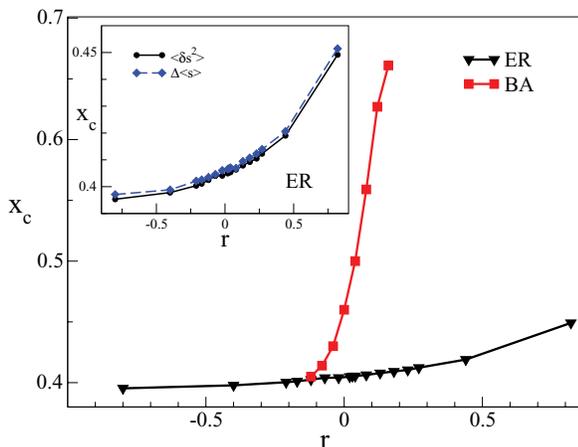


FIG. 8. (Color online) Comparison of the percolation thresholds $x_c$ for both the Erdős-Rényi and scale-free interacting networks. Scale-free networks exhibit a significant variation upon a small increase of the assortativity $r$, but Erdős-Rényi networks exhibit only a small variation over the whole possible range of assortativities. (Inset) The estimates of $x_c$ via the normalized increment $\Delta\langle s \rangle$ are very close to the estimates of $x_c$ via the peaks of $\langle (\delta s)^2 \rangle$ also for Erdős-Rényi networks.
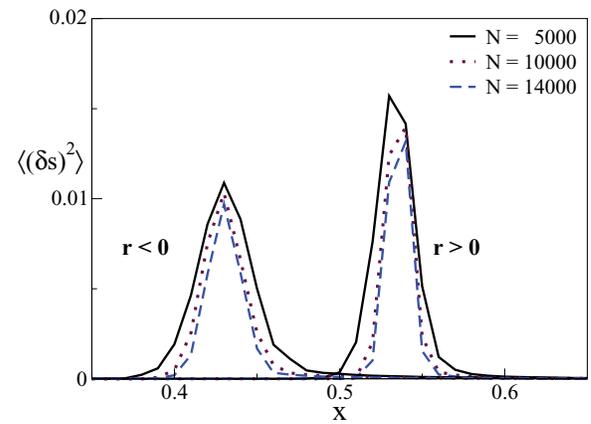


FIG. 9. (Color online) Fluctuations $\langle (\delta s)^2 \rangle$ of the order parameter $s$ as a function of the fraction $x$ of initially undamaged nodes for scale-free networks of different sizes. The peaks on the left correspond to disassortative networks ($J = -10$, i.e., $r$ from $-0.086$ to $0.051$) while the peaks on the right correspond to assortative networks ($J = 10$, i.e., $r = $ from $0.181$ to $0.163$). The different curves correspond to sizes $N = 5000$ (circles), $N = 10\,000$ (squares), and $N = 14\,000$. For the sizes analyzed, there is no significant evidence for the growth and narrowing of the peaks that would be expected in a second-order transition.

The second-largest cluster is found by following the algorithm II B but starting from the second-largest cluster (instead of the largest) at the first iteration. When we vary $x$ in our simulations we do not observe a peak in $s_2$. The size of the second-largest cluster is flat and always of order $\sim 1/N$. Therefore, all these arguments support the presence of a first-order transition as predicted by mean-field ER network-of-networks models [37,38].

Let us finally comment on the role of the hysteresis in signaling the order of the transition. In a first-order transition, local minima of the free energy develop before the transition point and become the favored ones at the transition point; on the same footings the local free-energy minimum corresponding to the equilibrium state before the transition persists as a metastable state for some range of the parameters. The switch of the favored minima at the transition point is signalled by a jump in any macroscopic quantities that discriminates among such minima; nevertheless, if minima are deep enough, the system can persist in the metastable state for a finite time before jumping to equilibrium. Such behavior results in hysteresis curves and is, therefore, linked to the equilibrium description of the system in terms of free energy. In the IFM there is no free-energy description of the system but a characterization of the final state as fixpoints of an operator: Therefore, the applications of statistical mechanics observables is just a guide to study the system; on the other hand, distinguishing the cases where the transition is abrupt (first order) is of great interest and importance for real systems.

## IV. CONCLUSION

We have examined the influence of assortativity on the robustness of interdependent systems consisting of two

interacting networks. Both SF and ER network models have been taken into account. The simulation of cascading faults caused by random attack or failure in the interdependent pair of networks provides evidence for a first-order percolation transition.

The percolation threshold decreases with increasing assortativity and, therefore, assortative networks are more fragile in both the ER and SF cases but, generally speaking, SF networks are less robust than ER interdependent pairs. Even a low assortativity can make a SF network 100% more fragile than its corresponding ER version.

[1] A. Berizzi, in *Power Engineering Society General Meeting, 2004. IEEE* (2004), Vol. 2, pp. 1673–1679.

[2] A. Usov, C. Beyel, E. Rome, U. Beyer, E. Castorini, P. Palazzari, and A. Tofani, in *Advances in System Simulation (SIMUL), 2010 Second International Conference on* (2010), pp. 121–128.

[3] R. Klein, E. Rome, C. Beyel, R. Linneman, W. Reinardt, and A. Usov, Lect. Notes Comput. Sci. **5508**, 36 (2009).

[4] W. Kröger and E. Zio, in *Vulnerable Systems* (Springer, London, 2011), pp. 55–64.

[5] C. D. Brummitt, R. M. DSouza, and E. A. Leicht, Proc. Natl. Acad. Sci. USA **109**, E680 (2012).

[6] S. V. Buldyrev, R. Parshani, G. Paul, H. E. Stanley, and S. Havlin, Nature **464**, 1025 (2010).

[7] Z. Wang, A. Szolnoki, and M. Perc, Europhys. Lett. **97**, 48001 (2012).

[8] S. Jolad, R. Zia, and B. Schmittmann, in *APS March Meeting 2012* (2012).

[9] M. Dickison, S. Havlin, and H. Stanley, in *APS March Meeting 2012* (2012).

[10] A. Saumell-Mendiola, M. A. Serrano, and M. Boguñá, Phys. Rev. E **86**, 026106 (2012).

[11] S.-W. Son, G. Bizhani, C. Christensen, P. Grassberger, and M. Paczuski, Europhys. Lett. **97**, 16006 (2012).

[12] A. Bashan, R. P. Bartsch, J. W. Kantelhardt, S. Havlin, and P. C. Ivanov, Nat. Commun. **3**, 702 (2012).

[13] D. E. Newman, B. Nkei, B. A. Carreras, I. Dobson, V. E. Lynch, and P. Gradney, in *Hawaii International Conference on System Sciences* (IEEE, 2005).

[14] G. Caldarelli, *Scale-free Networks* (Oxford University Press, 2007).

[15] A. Barrat, M. Barthélemy, and A. Vespignani, *Dynamical Processes on Complex Networks* (Cambridge University Press, Cambridge, UK, 2008).

[16] R. Pastor-Satorras and A. Vespignani, Phys. Rev. Lett. **86**, 3200 (2001).

[17] M. E. J. Newman, Phys. Rev. Lett. **89**, 208701 (2002).

[18] M. E. J. Newman, Phys. Rev. E **67**, 026126 (2003).

[19] A. Vázquez and Y. Moreno, Phys. Rev. E **67**, 015101 (2003).

[20] G. D'Agostino, A. Scala, V. Zlatíc, and G. Caldarelli, Europhys. Lett. **97**, 68006 (2012).

[21] M. Brede and S. Sinha, arXiv:cond-mat/0507710v1.

[22] R. M. May, *Stability and Complexity in Model Ecosystems (Princeton Landmarks in Biology)* (Princeton University Press, Princeton, NJ, 2001).

[23] P. V. Mieghem, *Graph Spectra for Complex Networks* (Cambridge University Press, Cambridge, UK, 2010).

[24] S. Maslov and K. Sneppen, Science **296**, 910 (2002).

[25] R. Xulvi-Brunet and I. M. Sokolov, Phys. Rev. E **70**, 066102 (2004).

[26] J. D. Noh, Phys. Rev. E **76**, 026116 (2007).

[27] S.-H. Yook and J. Park, Europhys. Lett. **93**, 38001 (2011).

[28] S. Zhou and R. J. Mondragón, New J. Phys. **9**, 173 (2007).

[29] R. Albert and A.-L. Barabási, Rev. Mod. Phys. **74**, 47 (2002).

[30] B. Bollobas, *Modern Graph Theory* (Springer, Berlin, 1998).

[31] J. Menche, A. Valleriani, and R. Lipowsky, Phys. Rev. E **81**, 046103 (2010).

[32] D. Stauffer and A. Aharony, *Introduction To Percolation Theory*, 2nd ed. (CRC Press, Boca Raton, FL, 1994).

[33] M. S. S. Challa, D. P. Landau, and K. Binder, Phase Transitions **24–26**, 343 (1990).

[34] R. A. da Costa, S. N. Dorogovtsev, A. V. Goltsev, and J. F. F. Mendes, Phys. Rev. Lett. **105**, 255701 (2010).

[35] N. Jan, D. Stauffer, and A. Aharony, J. Stat. Phys. **92**, 325 (1998).

[36] C. R. da Silva, M. L. Lyra, and G. M. Viswanathan, Phys. Rev. E **66**, 056107 (2002).

[37] J. Gao, S. V. Buldyrev, S. Havlin, and H. E. Stanley, Phys. Rev. Lett. **107**, 195701 (2011).

[38] J. Gao, S. V. Buldyrev, H. E. Stanley, and S. Havlin, Nat. Phys. **8**, 40 (2012).